SURFACE ROUGHNESS PREDICTION WITH DENOISING USING WAVELET FILTER

Syed Jahangir Badashah[1] and P.Subbaiah[2]
[1]Department of Electronics & Communication Engineering,
Research Scholar of Sathyabama University, Chennai., India
[2]Principal & Prof., ECE Dept,
Bharat College of Engineering & Technology for Women, Kadapa, AP, India

ABSTRACT

In today's competitive world, the best way to survive a company is to produce a good service and a quality product. One of the best way to monitor the surface quality of a machined part is to measure the surface roughness. Surface metrology with image processing is a challenging task having wide applications in industry. Surface roughness can be evaluated using prediction approach. Image denoising involves the manipulation of the image data to produce a visually high quality image. The filtering approach has been proved to be the best when the image is corrupted. The need for quality control and performance testing has become an integral part of the procedure. Surface finish plays an important role in several engineering applications like surface quality of any machined part, performance of good quality machined components and significantly improves fatigue strength, corrosion resistance, creep life etc.

KEYWORDS: *Surface roughness, Prediction, Wavelet transform, milling, grinding, noise removal filter.*

I. INTRODUCTION

The time-domain wavelets are plain oscillating amplitude functions of time. Wavelet representations rely on two fundamental factors i.e. Scaling and Translations. The composition of scaled and translated wavelets of the alike basic wavelet shape forms a wavelet family. The time or space resolution develops as the scale of a signal event decreases. The Wavelets are band-limited [1]. They are composed of many but a relatively limited range of several frequencies. They have huge fluctuating amplitudes during a limited time period and are very low amplitude or null amplitude outside of that time range. They are localized in both frequency and time [12]. They display sensitivity to full-scale range of waveform constitution. They offer effective time-frequency decomposition of signal over a range of characteristic frequencies that splits individual signal components.

This paper is organize as follows, section 2 discusses the degrees of freedom, section 3 related works, section 4 Surface roughness and its importance with specifications of operations, section 5 prediction model, section 6 methodology, section 7 noise removal schemes, section 8 results and discussions. Conclusion has been summarized end section 9.

II. DEGREES OF FREEDOM

In digital communication, applied mathematics and signal image processing areas have proposed and developed many diverse wavelet systems. The researchers are working actively in devising much new wavelets with specific characteristics. Different classes can be suggested to differentiate wavelets with respect to the kinds and ways of their representations. There are numerous interesting wavelets with infinite features and support [7]. Some of the infinite support wavelets are Gaussian wavelets, Mexican Hat, Morlet, and Meyer. Gaussian wavelets are obtained from the derivatives of the

Gaussian function. The subsequent mathematical analysis explains the degrees of freedom of wavelet analysis used in these techniques. The degrees of freedom include:

1. Levels: This value depends on the type of transform and characteristics of the frequency signal.
2. Function of basis Wavelet.
3. Type of Transform: This fixes two parameters namely decomposition and behavior of signal.

III. RELATED WORKS

[1] greater incidence of impulsive noise at the output similar to the case of five elements median filter is presented. The median filter will not correct an error unless at least three elements contain a wrong data.
[2] they evaluate the performance along with pre-processing techniques using wavelet transform applied to face images.
[3] a different treatment of regions with different homogeneity degree is presented. The use of such generalized model makes the treatment more precise but provides implicit solution for the MAP filter equation.
[4] describes different methodologies for noise reduction giving an insight as to which algorithm should be used to find the most reliable estimate of the original image data given its degraded version.
[5] a good review of the field, hopefully a fairly inclusive one, and at the same time trying to give some insight into the various classes of techniques for measuring surfaces and their uses is done.
[6] four methods that yield mathematical measures to analyze the precision of surfaces of manufactured parts is investigated. The average energy is given by the eigenvalues of the covariance matrix.
[7] includes intuitive properties like roughness, granulation and regularity. To obtain features which reflect scale-dependent properties, one can extract a feature from each sub image separately.
[8] they propose a combination of three texture descriptors namely Standard Deviation, Kurtosis and Canny edge detector. They used three texture databases namely Milling, Casting and Shaping.
[9] the texture analysis based on wavelet transformations is elaborated.
[10] they show that there is an interesting connection between wavelets and statistical properties of real-world images.
[11] a number of image analysis methods are presented as solutions to two applications concerning the characterization of materials.
[12] reports that the deeper a valley, the darker the corresponding pixel, the higher a peak, the brighter the corresponding area in the image.
[13] describes the new approach to construct the best tree on the basis of Shannon entropy. The proposed algorithm provides a good compression performance. Basis functions are obtained from a single photo type wavelet called the mother wavelet by dilation (scaling) and translation (shifts). These sets are divided into four parts such as approximation, horizontal details, vertical details and diagonal details. They have implemented the proposed algorithm, wavelet packet best tree using Shannon entropy.
[14] reported that contact type techniques have its own disadvantages such as workpiece surface damage due to mechanical contact between the stylus and the surface. In this context, the entire surface area for estimation surface roughness parameters using a multi layer perceptron (MLP) artificial neural network is discussed.

IV. SURFACE ROUGHNESS

4.1 Surface Roughness and its importance

The evaluation of surface roughness of machined parts using a direct contact method has limited flexibility in handling the different geometrical parts to be measured [11]. Surface roughness also affects several functional attributes of parts, such as friction, wear and tear, light reflection, heat transmission, ability of distributing and holding a lubricant, coating etc [8]. Therefore, the desired surface finish is usually specified and appropriate processes are required to maintain the quality [14]. Hence, the inspection of surface roughness of the work piece is very important to assess the quality of

a component [9]. Alternately, optical measuring methods are applied to overcome the limitations of stylus method, but, they are also sensitive to lighting conditions and noise. The technique proposed in this work, requires no apriority information about the lighting conditions and source of noise. It is important that the specification should include a 'maximum' transverse surface roughness requirement. Scanning Electron Microscopy (SEM) revealed that the samples with a high surface roughness are heavily damaged by the polishing operation[10], whilst those with low surface roughness are relatively undamaged, showing only light scoring of the surface[5][6]. Mean values of selected roughness parameters foreommon technological process are shown in Table 1.

Table 1 Mean value of roughness parameters

Machine	Roughness Parameters				
	Ra[µm]	Rz[µm]	RSm[µm]	Rλq[µm]	RΔq[*]
T	0.27±0.022	1.99±0.16	79.91±6.08	32.42±2.92	4.81±0.64
BG-30	0.13±0.010	1.24±0.10	29.29±1.85	18.42±0.96	3.91±0.28
BG-9	0.05±0.008	0.46±0.05	48.53±9.13	25.22±2.89	1.42±0.04

It can be observed from Table 1 that the mean values and confidence intervals of vertical and hybrid parameters values are decreasing with every step of technological process. However, the horizontal parameters change their values in a different way.

4.1.2 Surface Roughness Parameter (G_a)

An important feature of surface image that can be used to predict surface roughness is arithmetic average of gray levels, G_a. This parameter (G_a) is expressed in eqn. (1)

$$G_a = \frac{(\Sigma(|g_1 - g_m| + |g_2 - g_m| + \ldots\ldots + |g_n - g_m|)}{n} \ldots\ldots (1)$$

where, $g_1, g_2, g_3, \ldots, g_n$ are the gray level values of a surface image along one line and g_m is the mean of the gray values as given in eqn. (2)

$$g_m = \frac{\sum(g_1 + g_2 + \cdots + g_n)}{n} \ldots\ldots (2)$$

Quantification methods based on 2D parameters are well described by IS0 standards and by far are the most widely used. The description of the roughness measure is shown in figure 1.

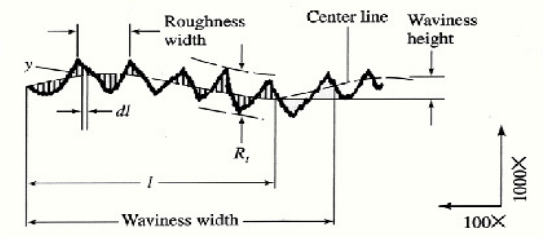

Figure 1. Roughness measures

4.2 Machine Vision based Image Acquisition and Processing

Image processed using a computer is digitized first, after which it may be represented by a rectangular matrix with elements corresponding to the brightness at appropriate image locations using machine vision approach. From the image vector, a rough surface can be understood as an image with the grey levels corresponding to the surface relief and deeper a valley, the darker the corresponding pixel. Similarly, the higher a peak is the brighter the corresponding area in the image. Texture analysis of these images (in order to characterize them) is still an open field, as there is no single technique that can be used to entirely characterize a texture.

4.2.1 Specification of Milling Operation

Experiments with different operating conditions (i.e., varying speed, feed, and depth of cut) are conducted on a milling process. The machining parameters used for milling are given in Table 2.The specifications of the milling machine is given in table 3,tool specifications in table 4 and composition of work piece in table 5.

Table 2 Machining Parameters

Tool	Speed (m/sec)	Feed (mm/min)	Depth of cut (mm)	Cutter diameter (mm)
Carbide	32-2000	40-1250	0.1-1.6	25

Table.3 Specifications of milling machine

Type	mm
Longitudinal	630
Cross feed	250
Height	450

Table 4. Tool specification

Tool type	Mm
Tool Diameter	25φ

Table 5 Composition of work piece

Material	Grade	C	Si	Mn	Co
EN8	SAE 1038	0.35%	0.10%	0.6%	0.06%

4.3 Roughness Estimation of Milled Components

4.3.1 Typical Milling Images

Typical images of the surface texture for milling along with their histogram are shown in Figure 2.

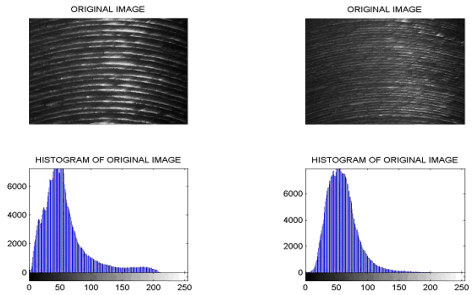

Figure 2 Typical Milled images with histogram

As inferred from Figure 2 there is a shift of the histogram towards higher grey levels as the surface becomes smoother i.e. the reflectivity increases, resulting in higher grey level values. The study of correlation between the gray levels and the surface roughness values provides a machine independent way of estimating the surface roughness.

V. PREDICTION MODEL

The prediction and regression analysis uses a set of tested methods that would analyze the data and distinguish patterns. This paper proposes a method a non-probabilistic binary linear model i.e. it predicts, for each given element of inputs, the surface roughness parameter. The task generally involves with training and testing data which consists of some data instances. Each instance in the training set contains one "target value" (class labels) and several "attributes" (features). The present predication has an additional advantage of automatic model selection in the sense that both the optimal number and locations of the basic functions are automatically obtained during training.

$$(x_i, y_i), i = 1 \ldots . . n, x \in R^n, y\{-1, +1\} \ldots . . (3)$$

For the input training sample set the prediction hyperplane equation is let to be

$$(\omega . x) + b = 0 \ldots \ldots \qquad \ldots \ldots \ldots \ldots \ldots (4)$$

thus the prediction margin is 2 / |ω| .To maximize the margin, that is to minimize |ω| the optimal hyperplane problem is transformed to quadratic programming problem as follows,

$$\begin{cases} min\emptyset(\omega) = 1(\omega, \omega)/2 \\ such\ that y_i((\omega . x) + b \geq 1, i = 1,2 \ldots l \end{cases} \quad \ldots \ldots (5)$$

After introduction of Lagrange multiplier, the dual problem is given by

$$\begin{cases} \max Q(\alpha) = \sum^{n} \alpha_{i} - \frac{1}{2}\sum_{i=1}^{n}\sum_{j=1}^{n} y_i y_j \alpha_i \alpha_j K(x_i . x_j \\ such\ that \sum_{i=1}^{n} y_i \alpha_i = 0, \alpha_i \geq 0, i = 1,2 \ldots . , n \ldots . (6) \end{cases}$$

According to Kuhn-Tucker rules, the optimal solution must satisfy

$$(y_i((w.x_i) + b) - 1 = 0, i = 1,2,..n \quad \ldots\ldots \quad (7)$$

That is to say if the option solution is

$$\alpha^* = (\alpha_1^*, \alpha_2^*, \ldots\ldots, \alpha_i^*)^T, i = 1,2, \ldots . n \ \ldots . . (8)$$

Then $w^* = \sum_{i=1}^{n} \alpha_i^* y_i x_i$

$$b^* = y_i - \sum_{i=1}^{n} y_i \alpha_i^* (x_i, x_j), j \in \{j | \alpha_i^* > 0 \ \ldots . . (9)$$

For every training sample point x_i, there is a corresponding Lagrange multiplier. And the sample points that are corresponding to$\alpha_i = 0$ don't contribute to solve the prediction hyperplane while the other points that are corresponding to $\alpha_i > 0$ do, so it is called support vectors. Hence the optimal hyperplane equation is given by,

$$\sum_{x,\in sv} \alpha_i y_i (x_i . x_j) + b = 0 \qquad (10)$$

The hard predictor is then, $y = sgn[\sum_{x,\in sv} \alpha_i y_i (x_i, x_j) + b\ ] \ \ldots . \quad (11)$

For nonlinear situation, it is required to construct an optimal separating hyperplane in the high dimensional space by introducing kernel function $K(x.y) = \emptyset(x).\emptyset(y).$*Hence* the nonlinear predictor is given by,

$$\begin{cases} min \emptyset(\omega) = 1(\omega, \omega)/2 \\ such\ that y_i((\omega.\emptyset(x_i)) + b \geq 1, i = 1,2 \ldots l \end{cases} \quad (12)$$

And its dual problem is given by,$\begin{cases} maxL(\alpha) = \sum_{i=1}^{l} \alpha_i - \frac{1}{2}\sum_{i=1}^{l}\sum_{j=1}^{l} y_i y_j \alpha_i \alpha_j K(x_i . x_j) \\ such\ that \sum_{i=1}^{n} y_i \alpha_i = 0, 0 \leq \alpha_i \leq C, i = 1,2, \ldots l \ldots (13) \end{cases}$

Thus, the optimal hyperplane equation is determined by the solution of the optimal problem.

VI. RESEARCH METHODOLOGY

The surface roughness related parameters are to be computed as a basic prerequisite of the experiment. In order to remove artifacts from the measured sensor values Wavelet based novel filter is used, and a predictor (multi objective) based on the filtered surface roughness related features coexist as shown in figure 3. This integrates the predictor output and performs surface roughness estimation.

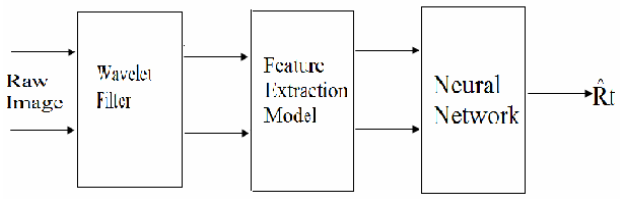

Figure 3. Block diagram.

A filtering process is to be used to establish a three-dimensional reference surface consisting of waviness and form errors and the roughness component needs to be separated with reference to it. The Wavelet technique in this work, used for profile/surface analysis, exploits the waviness transmission characteristics through the wavelet decomposition filters and the feature extraction technique does not contain any machined parameter component. This differs from previous reported works, where the feature extraction technique contains some transformed features along with machined parameters.

Thus, the advantage of the presented feature extraction technique is that, it can be adapted generically in any machine vision applications. In this work, the multi-layer perceptron neural network with back propagation as the training algorithm is employed and the neural network is trained with selected significant patterns for the effective prediction of surface roughness of machined components[2].

VII. NOISE REMOVAL SCHEMES

The noise elimination strategies suited for sensor noise cancellation in a real time environment favors a noise cancellation model in which the secondary noise source $n_2(k)$ is absent[3], while retaining the constraints that

(i) $x(k)$ and $n_1(k)$ can be non-stationary and

(ii) no apriori statistical information is required about $x(k)$ and $n_1(k)$.

7.1 Proposed Noise Removal filter (NRF) and its Advantages

This network architecture is shown in Figure 4. The delay path serves to generate a reference signal, that can be used to estimate $x(k)$. No apriori statistical information about the desired signal is required to be given as input to the network. Also, the source signal $x(k)$ need not be stationary.

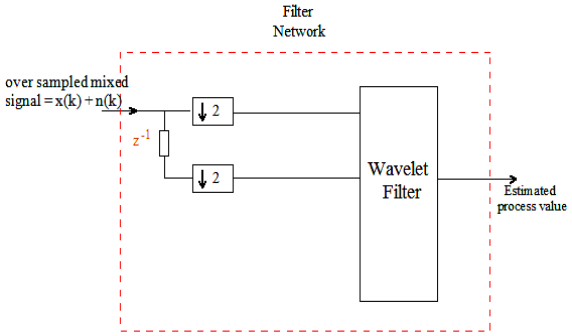

Figure. 4 Adaptive noise cancellation network for non-stationary signals with no secondary noise source

7.2 Design of Wavelets Based Filter

The wavelets having same vanishing moments and same length of phase factor with different frequencies is designed and also compared with standard filter design response. The measure of smoothness of wavelet is obtained by Sobolev regularity s_c by using eigenvalue approach [4]. This approach is different from other types of least squares approaches for FIR design, which are obtainable by matrix inversion. The advantages of eigenfilters over other FIR filter (such as equiripple filters) is that, it can be designed to incorporate a wide variety of time domain constraints such as the step response constraint, Nyquist constraint and so on[13], in addition to the usual frequency domain requirements. The filter coefficients are obtained simply by computing eigenvector of a positive definite matrix, which is derived from the time and frequency domain specifications. Eigen filters can be used for optimal design of the so called Nyquist filters, which are ideally suited for interpolation filtering. The spectrum of complex wavelet is shown in Figure 5 wherein for comparison the equiripple case spectrum is also shown.

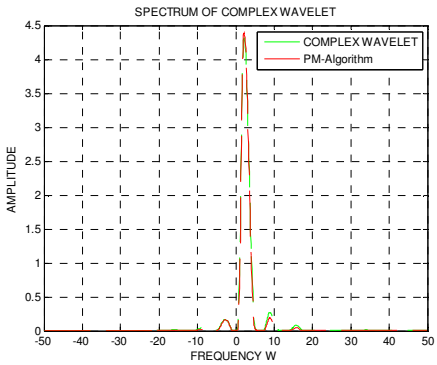

Figure 5 Spectrum of complex wavelet (proposed and in equiripple method)

7.3 Performance Metric

The low pass filter of filter bank denoted by $H^h(Z)$ and $H^g(Z)$ should satisfy the half sample delay condition

$$H^g(z) = e^{\frac{-jw}{2}} H^h\left(e^{jw}\right)$$
$$for -\pi \le w \le \pi \ \ldots\ldots \qquad (14)$$

The spectrum of complex wavelet is defined as $\Psi^A(t) = \Psi^h(t) + j\Psi^g(t)$ is ideally complex analytic, the spectrum satisfy

$$\Psi^A(w) = \Psi^h(w) + j\Psi^g(w) = 0$$

for w<0. The strict complex analyticity cannot be achieved.

7.3.1 Quality measure of Wavelet filter

The quality measures of wavelet denoted by,

$$E_1 \equiv \frac{Max_{w<0|}|\Psi^A(w)|}{Max_{w>0}|\Psi^A(w)|} \quad E_2 \equiv \frac{\int_{-\infty}^{0}|\Psi^A(w)|^2 dw}{\int_{0}^{\infty}|\Psi^A|(w)|^2 dw} \ldots (15)$$

E1 and E2 measure the peak energy and negative frequency energy respectively. The lower values give better quality of wavelets.

7.3.2 Design Procedure

Step 1: Formulate the coefficient b_n where amplitude response

$$H_R(w) = \sum_{n=0}^{M} b_n coswn = b^T c(W)$$

Step 2: Assign $b_{Mn} = \begin{cases} c & n = 0 \\ 0 & n \neq o \end{cases}$

to obtain M^{th} band condition

Step 3: Minimize the objective function $\Phi = b^T Rb, \qquad R = \alpha p + (1-\alpha) Q$

where R is real, symmetric and positive.

Step 4: Choose optimum vector 'b' = eigvect ® corresponding to its smallest eigen value λ_0. The stability of designed filter is established in appendix 1.

VIII. RESEARCH RESULTS AND DISCUSSION

The results obtained by using the wavelet based image enhancement filter are presented in this section. Table 6 and Table 7 show the PSNR improvement obtained by using the wavelet based image enhancement for both milling and grinding process. The histogram of original image and filtered image is shown in figure 6 and figure 7 for two sample cases. It can be inferred from table 6 and table 7 that among all the approaches used to enhance image quality using computer vision, application of wavelet techniques to the grabbed image was found to be the more effective. Hence, this technique can be efficiently used for non-contact inspection of components, which has assumed considerable significance. The estimation of G_a (optical roughness value) after applying wavelet technique had a better correlation (i.e. higher correlation coefficient) with the average surface roughness (R_t) measured using a conventional and widely accepted stylus type instrument for the components manufactured particularly using milling and grinding processes. Also, the PSNR value is found to be best in the wavelet based scheme. The higher PSNR indicates a better resolution and degradation and blurring of edges gets removed to a large extent. It is worth mentioning that this improvement is significant for the milled surfaces compared to the ground surfaces. This trend can be explained from the fact that there is a large local variation in the characteristic of ground surface, as compared to the more uniform and fine milled surfaces resulting in better correlation between stylus R_t and vision roughness R_t for milled surfaces.

Table 6. Results of the different super-resolution algorithms on the surface images (Milled surfaces)
surfaces)

S.No	Speed (m/s)	Depth of cut (mm)	Feed (mm/sec)	PSNR (dB)			R_t (µm)
				1	2	3	
1	10.04	25	0.2	16.865	18.362	24.362	25.17
2	14.13	11.2	0.4	17.94	17.98	18.94	21.85
3	19.78	16	0.2	24.59	26.54	30.21	19.47
4	28.26	16	0.2	30.64	32.46	32.64	23.34
5	39.25	22.4	0.8	28.54	29.47	31.24	27.65
6	56.25	31.5	0.4	18.64	17.58	19.17	24.67
7	78.5	45	0.4	33.64	35.54	36.34	24.1
8	111.5	63	1	16.59	18.24	19.347	27.26

Note: 1- Vandewalle approach 2 - Keren approach 3Wavelet Algorithm Algorithm

Table7 Results of the different super resolution algorithms on the surface images (Grinding

S.No	Speed (m/s)	Depth of cut (mm)	Feed (mm/rev)	PSNR (dB)			R_t (µm)
				1	2	3	
1	36.63	5	20	24.103	24.168	28.329	2.686
2	36.63	10	20	22.65	30.21	32.12	2.568
3	39.25	10	10	20.18	24.21	27.56	2.731
4	39.25	15	25	18.95	23.64	25.24	2.898
5	36.63	15	10	17.24	23.24	23.45	3.14
6	32.71	15	25	15.64	25.48	28.21	3.205
7	32.71	20	5	15.48	18.57	20.26	3.628
8	26.17	20	5	27.54	26.36	29.32	3.977

Note: 1- Vandewalle approach 2 - Keren approach 3Wavelet

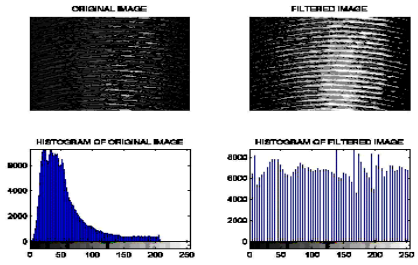

Figure 6. Histogram of the original and wavelet filtered filtered image (Milling).

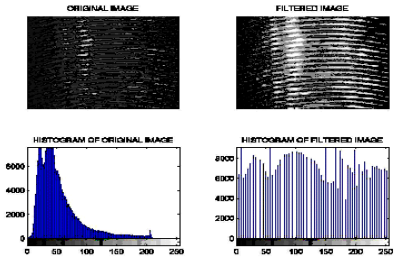

Figure7. Histogram of the original and wavelet wavelet filtered image (Grinding).

IX. CONCLUSION

The advantages of the present approach are the non-contact measurements and ease of automation. This work has described the use of machine vision techniques to inspect the surface roughness of a work piece under various milling and grinding operations. The image enhancement algorithm presented in this work is unique, and is ideally suited for a real time environment, where no apriori information is available about the noise mixed with the captured image. In comparison to conventional non-adaptive filters (which perform well only as long as the spatial density of the impulse noise is less), the wavelet based filter presented in this work can handle impulse noise even with higher probabilities and also can preserve sharpness and detail while smoothing non-impulse noise. Conventional filtering schemes may employ various image filters for different scenarios but it is very difficult and time consuming to find a set of appropriate filters and as a result most of them are suited for off-line implementation only. On the contrary, the proposed structure has the advantage that it does not require any expert knowledge to find the type and order of filters for a given domain.

REFERENCES

[1] Jaime Ramírez-Angulo, " A Restrained Neighborhood Analog Median Filter For Image Processing Applications " , Alejandro Díaz-Sánchez National Institute for Astrophysics, Optics and Electronics, Tonantzintla, Puebla, Mexico, New Mexico State University. Las Cruces, New Mexico, USA.
[2] Fan Yang, Michel Paindavoine, "A New Image Filtering Technique Combining aWavelet Transform with a Linear Neural Network : Application to Face Recognition ", Universit´ e de Bourgogne, France, The University of Texas at Dallas Program in Cognition, U.S.A., 2000.

[3] Alexandru Isar, Sorin Moga, Dorina Isar, "Image Denoising Using a Bishrink Filter with Reduced Sensitivity ", "Politehnica" University, Timisoara, Romania, Brest, France.
[4] Mukesh C. Motwani, Mukesh C. Gadiya, Rakhi C. Motwani, Frederick C. Harris, Jr., "Survey of Image Denoising Techniques ", Image Process Technology, Back Country Road, USA, University of Pune, India, University of Nevada, USA.
[5] T.V. Vorburger, J. Raja, " Surface Finish Metrology Tutorial ", U.S. Department of Commerce, National Institute of Standards, USA, 1990.
[6] Irem Y. Tumer, R.S. Srinivasan, Kristin L. Wood, " Characteristic Measures for the Representation of Manufactured Surface Quality ", ASME design Engineering Technical Conference and Design for Manufacturing Conference, Irvine, California, August (18-22) 1996.
[7] S.Livens, P.Scheunders, G.Van de Wouwer, D.Van Dyck, " Wavelets for Texture Analysis ", University of Antwerp, Belgium, 30th June 1997.
[8] Smriti H. Bhandari, S. M. Deshpande, "Feature Extraction for Surface Classification –An approach with Wavelets ", International Journal of Computer and Information Science and Engineering.
[9] P.Scheunders, S.Livens, G. Van de Wouwer, P.Vautrot, D.Van Dyck, " Wavelet-based Texture Analysis ", University of Antwerp, Belgium, 1997. [10] Jarmo Hurri, Aapo Hyvärinen, Erkki Oja,"Wavelets and Natural Image Statistics ", Helsinki University of Technology, Espoo, Finland, 1997.
[11] Stefan Livens, " Image Analysis for Material Characterization ", University of Antwerp, Belgium, 1998.
[12] Bruno Josso , David R. Burton, Michael J. Lalor, "Frequency normalised wavelet transform for surface roughness analysis and characterisation ", Liverpool John Moores University, Liverpool, UK, 10th January 2002.
[13] G. K. Kharate, A. A. Ghatol, P.P. Rege, "Image Compression Using Wavelet Packet Tree ", K.K.Wagh Institute of Engineering Education and Research, Maharashtra, India, July 2005.
[14] Dr Colin Honess, " Importance of Surface Finish in the Design of Stainless Steel ", Swinden Technology Centre, August 2006

APPENDIX-I

We are given that $H_0(z) = \frac{P_0(z)}{D(z)}$, $H_1(z) = \frac{P_1(z)}{D(z)}$ and the following properties:

(i) $\tilde{P}_o(z)=z^N P_o(z)$,
(ii) $\tilde{P}_1(z)=cz^N P_1(z)$ for $|c|=1$, and
(iii) $\tilde{H}_o(z)H_o(z)+\tilde{H}_1(z)H_1(z)=1$.

Substituting $H_o(z)$ and $H_1(z)$ into property (iii), we get

$\tilde{P}_o(z)P_o(z)+\tilde{P}_1(z)= \tilde{D}(z)D(z)$.

Using property (i) and (ii) ,we get $z^n P_0^2(z) + cz^N P_1^2(z) = \tilde{D}(z)D(z)$.

Since $|c|=1$,we can represent it as $c=e^{j\theta}$. Thus, we can rewrite the above equation as

$[P_o(z)+je^{j\theta/2} P_1(z)][P_o(z)-je^{j\theta/2} P_1(z)]=z^N\tilde{D}(z)D(z)$. .....eq(1)

Since $H_o(z)$ and $H_1(z)$ are stable, $D(z)$ has all zeros inside the unit circle,and $z^N\tilde{D}(z)$ has all zeros outside the unit circle. Therefore, the RHS (hence the LHS) of …eq(1) does not have zeros on unit circle.Suppose $P_o(z)+je^{j\theta/2} P_1(z)$ has n_1 zeros inside the unit circle, and $n_0 = N-n$ zeros outside the unit circle.Then,we can write

$P_o(z)+je^{j\theta/2} P_1(z)=\beta D_1(z)z^{-no}\tilde{D}_o(z)$ .....eq(2)

Where $D_o(z)=1+\sum_{n=1}^{no} d_{o,n}z^{-n}$ and $D_1(z)= 1+\sum_{n=1}^{n1} d_{1,n}z^{-n}$.$D_1(z)$ contains n_1 zeros inside the unit circle and $z^{-no}\tilde{D}_o(z)$ contains all the n_o zeros outside the unit circle. Then …eq(2)

$\Longrightarrow \tilde{P}_o(z)-je^{-j\theta/2} \tilde{P}_1(z)=\beta^*\tilde{D}_1(z)z^{no}D_o(z)$

$\Longrightarrow z^N P_o(z)-je^{-j\theta/2} cz^N P_1(z)=\beta^*\tilde{D}_1(z)z^{no}D_o(z)$ .....eq(3)

$\Longrightarrow P_o(z)-je^{j\theta/2} P_1(z)= \beta^*\tilde{D}_1(z)z^{-n1}D_o(z)$

From eq(1),eq(2) and eq(3),we can conclude

$z^{-N}\tilde{D}(z)\,D(z) = |\beta|^2 z^{-N}\tilde{D}_1(z)\,\tilde{D}_0(z)\,D_1(z)\,D_0(z)$.

we know $D(z)$ has N zeros inside the unit circle, and $D_0(z)$, $D_1(z)$ have n_o,n_1 zeros inside the unit circle, respectively. Therefore, we know that $D(z)= D_0(z)\,D_1(z)$,and $|\beta|=1$.Dividing eq(2) and eq(3) by $D(z)$,we get

$$= \beta \frac{z^{-n_0}\widetilde{D}o(z)}{Do(z)} \frac{P_0(z) + je^{j\frac{\theta}{2}}P_1(z)}{D(z)} = \frac{P_0}{D(z)} + je^{j\frac{\theta}{2}}\frac{P_1(z)}{D(z)} = H_0(z) + je^{j\frac{\theta}{2}}H_1(z),$$

and $\beta^* \frac{z^{-n_1}\widetilde{D}1\,(z)}{D_1(z)} = \frac{P_0(z) - je^{j\frac{\theta}{2}}P_1(z)}{D(z)} = \frac{P_0(z)}{D(z)} - je^{j\frac{\theta}{2}}\frac{P_1(z)}{D(z)} = H_0(z) - je^{j\frac{\theta}{2}}H_1(z)$

Let $A_0(z) = \frac{z^{-n_0}\widetilde{Do}(z)}{Do(z)}$, and $A_1(z) = \frac{z^{-n_1}\widetilde{D}1(z)}{D_1(z)}$.

It is clear that $A_o(z)$ and A_1 are unit magnitude, all pass, and stable. Then, we can obtain

$$H_0(z) = (\beta A_0(z) + \beta^* A^1(z))/2$$
$$H_1(z) = d\frac{\beta A_0(z) - \beta^* A_1(z)}{2}$$

Where $d = -je^{-j\theta/2}$,so $|d| = 1$

Biographies

Syed Jahangir Badashah received B.E. degree in Electronics & Communication Engineering from Gulbarga University, in 2002,M.E.in Applied Electronics from Sathyabama University in 2005.He is currently doing research in image processing from Sathyabama University. He is having an experience of 10 years, in the field of teaching, presently working as S.G. Assistant Professor in the department of ECE, Madina Engg College, Kadapa. He is a life time member of IETE & ISTE.

P. Subbaiah, has received his M.Tech in Radar Engg from S.V. University, he also done M.Tech in DSCE from JNT University. He completed his research work from Instrumentation background. He is having more than 18 years teaching experience. He is presently working as Principal in Bharat College of Engineering & Technology For Women, Kadapa, AP. His area of interest are Image processing, Fuzzy logic, Computer Networks, VLSI, Neural networks etc. He has several papers in national, International Journals and Conferences to his credit. He has acted as a judge for International conference and also conducted International conferences.